The Neutrinoless Double Beta Decay: The Case for Germanium Detectors *

A. Morales† and J. Morales
Laboratory of Nuclear Physics and High Energy Physics. Faculty of Science, University of Zaragoza, Pedro Cerbuna 12, 50009 Zaragoza, Spain

1. Motivation and Introduction

In the Standard Model of Particle Physics neutrinos are strictly massless, although there is no theoretical reason for such prejudice. However, there exists conclusive experimental evidence that the neutrino has a non-zero mass, as deduced from the neutrino flavour oscillation observed in atmospheric and solar neutrino experiments. On the other hand, galaxy formation requires the presence (although small) of hot, non-baryonic dark matter particles, like non-zero mass neutrinos to match the observed spectral power.

In the Standard Model, neutrinos and antineutrinos are supposed to be different particles, but no experimental proof has been provided so far. The nuclear double beta decay addresses both questions: whether the neutrino is self-conjugated and whether it has a Majorana mass. The most direct way to determine if neutrinos are Majorana particles is to explore, in potential nuclear double beta emitters (A, Z), if they decay without emitting neutrinos $\rightarrow$ (A, Z+2) + $2e^-$, violating the lepton number conservation. For this non-standard $2\beta0\nu$ process to happen, the emitted neutrino in the first neutron decay must be equal to its antineutrino and match the helicity of the neutrino absorbed by the second neutron. Phenomenologically that implies the presence of a mass term or a right-handed coupling. A well-known argument of Schechter and Valle [1] shows that in the context of any gauge theory, whatever mechanism be responsible for the neutrinoless decay, a Majorana neutrino mass is required. Moreover [2], the observation of a $2\beta0\nu$ decay implies a lower bound for the neutrino mass, i.e. at least one neutrino eigenstate has a non-zero mass.

Another form of neutrinoless decay, (A, Z) $\rightarrow$ (A, Z+2) + $2e^-$ + χ may reveal also the existence of the Majoron (χ), the Goldstone boson emerging from the spontaneous symmetry breaking of B–L, of most relevance in the generation of Majorana neutrino masses and of far-reaching implications in Astrophysics and Cosmology. Moreover, current neutrino physics results have put on the front-line the double beta decay issue as a probe to explore and elucidate important open questions left unanswered by the oscillation experiments, namely the determination of the absolute mass scale.

In fact, the recent results of neutrino oscillation experiments indicate that next generation neutrinoless DBD experiments (besides answering the long standing question of the Majorana nature of neutrinos and the lepton number non-conservation) will provide information on the type of mass spectrum, the absolute neutrino mass scale and possibly the CP violation [3]. The data from Super-K, SNO as well as from a large body of previous neutrino oscillation experiments (Homestake, GALLEX, SAGE, Kamiokande), together with their theoretical analysis, clearly imply that neutrinos have indeed non-zero masses. However, neutrino oscillation experiments determine only the mass squared differences. Most of the models conclude that next-generation DBD experiments with mass sensitivities of the order of 10 meV may found the Majorana neutrino with a non-zero effective electron neutrino mass, if the

*Invited contribution at the XXX International Meeting on Fundamental Physics, IMFP2002, February 2002, Jaca, Spain.
†amorales@posta.unizar.es

neutrino is selfconjugate and the neutrino mass spectrum is of the quasi-degenerate type or it has inverted hierarchy. Majorana massive neutrinos are common predictions in most theoretical models, and the value of a few 10^{-2} eV predicted for its effective mass, if reached experimentally -as expected- will test its Majorana nature. DBD experiments with even better sensitivities (of the order of meV) will be essential to fix the absolute neutrino mass scale and possibly to provide information on CP violation.

Neutrinoless DBD are extremely rare processes. Their experimental investigation require a large amount of DBD emitter, in low-background detectors with capability for selecting reliably the signal from the background. Detectors should have a sharp energy resolution, or good tracking of particles, or other discriminating mechanisms. There are several natural and enriched isotopes that have been used in experiments with tens of kilograms. Some of them could be produced in amounts large enough to be good candidates for next generation experiments. The choice of the emitters should be made also according to its two-neutrino half-life (which could limit the ultimate sensitivity of the neutrinoless decay), according to its nuclear factor-of-merit and according to the experimental sensitivity that the detector can achieve in the case that the emitter is, at the same time, the detector. For obvious reasons it is important to explore various emitters and different techniques. Finally the extremely low background required for high sensitivity double beta decay searches requires to develop techniques for identifying, reducing and suppressing the background of all types and origins in the detectors and their environments . All these conditions set the strategies to search for the neutrinoless double beta decay.

The expected signal rate depends on the nuclear matrix element but the dispersion of results of the current calculations makes uncertain the interpretation of the experimental output. Improvements of the precision in theoretical evaluations of the matrix elements are essential. Experimental studies of nuclear structures, relevant to DBD, will help to perform adequate calculations of the matrix elements. The exploration of the conventional two-neutrino double beta decay of several potential double beta emitters and its comparison with theory must serve to help in determining the most suitable nuclear model. That improvements will hopefully provide accurate nuclear matrix elements for the neutrinoless DBD which are crucial for extracting the effective Majorana mass parameter.

In this talk we will sketch the guidelines in the search for double beta decay, in particular in the neutrinoless channel, and illustrate the strategies by choosing the case of germanium detectors, used in double beta searches as early as 1967. The neutrino effective mass bound has been steadily decreasing along the last decades, the stringent bound being provided by the germanium experiments. Consequently we will put the emphasis in the perspectives of the Ge^{76} case for reaching the ten (and less) millelectronvolt scale for the effective neutrino Majorana mass in the next generation experiments.

The paper is organized as follows: Section 2 will resume the main expressions for the half lives and mass bounds. Section 3 will describe the experimental strategies. Section 4 will describe the Ge experiments and give a comprehensive Table of the current situation with other emitters. Also the bounds of the Majorana effective neutrino mass will be shown. Finally Section 5 will present the current prospects with Ge-emitters as an example to illustrate the quest for the millielectronvolt mass sensitivity.

2. The Double beta decay modes

The two-neutrino decay mode (A, Z) $\rightarrow$ (A, Z+2) + $2e^-$ + $2\overline{\nu}_e$ is a conventional [2], although rare, second order weak process ($2\beta 2\nu$), allowed within the Standard Model. The half-lives are customary expressed as $[T^{2\nu}_{1/2}\ (0^+ \rightarrow 0^+)^{-1} = G_{2\nu} \mid M^{2\nu}_{GT} \mid^2$, where $G_{2\nu}$ is an integrated kinematical factor [4] and $M^{2\nu}_{GT}$ the nuclear double Gamow Teller matrix element.

The neutrinoless decay half-life (as far as the mass term contribution is concerned) is expressed as $(T^{0\nu}_{1/2})^{-1} = F_N \langle m_\nu \rangle^2 / m_e^2$. $F_N \equiv G_{0\nu} \mid M^{0\nu} \mid^2$ is a nuclear factor-of-merit and $M^{0\nu}$ is the neutrinoless nuclear matrix-element, $M^{0\nu} = M^{0\nu}_{GT} -$

$(g_V/g_A)^2\ M_F^{0\nu}$, with $M_{GT,F}^{0\nu}$ the corresponding Gamow-Teller and Fermi contributions. $G_{0\nu}$ is an integrated kinematic factor [4]. The quantity $\langle m_\nu \rangle = \Sigma \lambda_j m_j U_{ej}^2$ is the so-called effective neutrino mass parameter, where U_{ej} is a unitary matrix describing the mixing of neutrino mass eigenstates to electron neutrinos, λ_j a CP phase factor, and m_j the neutrino mass eigenvalue.

Concerning the neutrino mass question, the discovery of a $2\beta0\nu$ decay will tell that the Majorana neutrino has a mass equal or larger than $\langle m_\nu \rangle = m_e/(F_N T_{1/2}^{0\nu})^{1/2}$ eV, where $T_{1/2}^{0\nu}$ is the neutrinoless half life. On the contrary, when only a lower limit of the half-life is obtained (as it is the case up to now), one gets only an upper bound on $\langle m_\nu \rangle$, but not an upper bound on the masses of any neutrino. In fact, $\langle m_\nu \rangle_{exp}$ can be much smaller than the actual neutrino masses. The $\langle m_\nu \rangle$ bounds depend on the nuclear model used to compute the $2\beta0\nu$ matrix element. The $2\beta2\nu$ decay half-lives measured till now constitute bench-tests to verify the reliability of the nuclear matrix element calculations which, obviously, are of paramount importance to derive the Majorana neutrino mass upper limit. As stated in the Introduction the wide spread of the nuclear matrix elements calculation for a given emitter is the main source of uncertainty in the derivation of the neutrino mass bound. In the case of ^{76}Ge we quote the $2\beta0\nu$ nuclear merits $F_N^{0\nu}(y^{-1})$, according to various nuclear models (see Table 1).

Table 1
$2\beta0\nu$ nuclear merits $F_N^{0\nu}(y^{-1})$, according to various nuclear models

Ref.	$F_N^{0\nu}(y^{-1})$	Ref.	$F_N^{0\nu}(y^{-1})$
[5]	1.12×10^{-13}	[11]	7.33×10^{-14}
[6]	1.12×10^{-13}	[12]	1.42×10^{-14}
[7]	1.87×10^{-14}	[13]	5.8×10^{-13}
[8]	1.54×10^{-13}	[14]	1.5×10^{-14}
[9]	1.13×10^{-13}	[15]	9.5×10^{-14}
[10]	1.21×10^{-13}		

3. Searching for Double Beta Decays: Guidelines

The experimental signatures of the nuclear double beta decays are in principle very clear: In the case of the neutrinoless decay, one should expect a peak (at the $Q_{2\beta}$ value) in the two-electron summed energy spectrum, whereas two continuous spectra (each one of well-defined shape) will feature the two-neutrino and the Majoron-neutrinoless decay modes (the first having a maximum at about one third of the Q value, and the latter shifted towards higher energies). In spite of such characteristic imprints, the rarity of the processes under consideration make very difficult their identification. In fact, double beta decays are very rare phenomena, with two-neutrino half-lives as large as 10^{18} y to 10^{24} y and with neutrinoless half-lives as long as 10^{25} y (and beyond), as the best lower limit stands by now. Such remotely probable signals have to be disentangled from a (much bigger) background due to natural radioactive decay chains, cosmogenic-induced activity, and man-made radioactivity, which deposit energy on the same region where the 2β decays do it but at a faster rate. Consequently, the main task in 2β-decay searches is to diminish the background by using the state-of-the-art ultralow background techniques and, hopefully, identifying the signal.

To measure double beta decays three general approachs have been followed: geochemical, radiochemical and direct counting measurements. In the geochemical experiments, isotopic anomalies in noble gases daughter of 2β decaying nucleus over geological time scales are looked for. Determination of the gas retention age of the ore is important. They are inclusive $2\nu+0\nu$ measurements, not distinguishing 2ν from 0ν modes.

However, when $T_{1/2,exp.meas.}^{2\nu+0\nu(geoch.)} \ll T_{1/2,exp.bound}^{0\nu(direct)}$, most of the decay is through 2ν mode. The finite half-lives measured geochemically in the cases of ^{82}Se, ^{96}Zr, ^{128,130}Te, ^{238}U can be regarded as $2\beta2\nu$ half-life values. Also the $T_{1/2}$ values measured geochemically can be taken as a bound for $T_{1/2}^{0\nu}$, because $T_{1/2}^{0\nu}$ (or the half-life of whatever decay mode) cannot be shorter than $T_{1/2,exp.}$. Consequently, bounds on $\langle m_\nu \rangle$ can be derived from

geochemical half-life measurements.

Another way to look for double beta decays are the radiochemical experiments, by noticing that when the daughter nuclei of a double beta emitter are themselves radioactive, they can be accumulated, extracted and counted. If the daughter has a half-life much smaller than 10^9y and has no other long-lived parents, its presence can be only due to 2β. Parent minerals must have been isolated before 1940. Noticeable examples are that of $^{238}U \rightarrow {}^{239}Pu$ (88 y, α decay) and $^{244}Pu \rightarrow {}^{244}Cm$ (18 y, α decay).

Most of the recent activity, however, refers to direct counting experiments, which measure the energy of the 2β emitted electrons and so the spectral shapes of the 2ν, 0ν, and $0\nu\chi$ modes of double beta decay. Some experimental devices track also the electrons (and other charged particles), measuring the energy, angular distribution, and topology of events. The tracking capabilities are essential to discriminate the 2β signal from the background. The types of detectors currently used are:

- Calorimeters where the detector is also the 2β source (Ge diodes, scintillators – CaF_2, $CdWO_4$–, thermal detectors, ionization chambers). They are calorimeters which measure the two-electron sum energy and discriminate partially signal from background by pulse shape analysis (PSD). Notable examples of calorimeters are IGEX, H/M and MIBETA.

- Tracking detectors of source≠detector type (Time Projection Chambers TPC, drift chambers, electronic detectors). In this case, the 2β source plane(s) is placed within the detector tracking volume, defining two –or more– detector sectors. Leading examples of tracking devices are the NEMO series and ELEGANTS

- Tracking calorimeters: They are tracking devices where the tracking volume is also the 2β source, for example a Xenon TPC.

Well-known examples of 2β emitters measured in direct counting experiments are ^{48}Ca, ^{76}Ge, ^{96}Zr, ^{82}Se, ^{100}Mo, ^{116}Cd, ^{130}Te, ^{136}Xe, ^{150}Nd.

The strategies followed in the 2β searches are varied. Calorimeters of good energy resolution and almost 100% efficiency (Ge-detectors, Bolometers) are well suited for 0ν searches. They lack, obviously, the tracking capabilities to identify the background on an event-by-event basis but they have, in favour, that their sharp energy resolution do not allow the leakage of too many counts from ordinary double beta decay into the neutrinoless region, and so the sensitivity intrinsic limitation is not too severe. The identification capabilities of the various types of chambers make them very well suited for 2ν and $0\nu\chi$ searches. However, their energy resolution is rather modest and the efficiency is only of a few percent. Furthermore, the ultimate major background source in these devices when looking for $2\beta0\nu$ decay will be that due to the standard $2\beta2\nu$ decay. The rejection of background provided by the tracking compensates, however, the figure of merit in 0ν searches.

Modular calorimeters can have reasonable amounts of 2β emitters (Heidelberg/Moscow, IGEX, MIBETA and CUORICINO experiments) or large quantities (like CUORE and Majorana). Tracking detectors, instead, cannot accommodate large amounts of 2β emitters in the source plate. Recent versions of tracking devices have 10 kg and more (NEMO3).

The general strategy followed to perform a neutrinoless double beta decay experiment is simply dictated by the expression of the half-life ($T^{0\nu}_{1/2} \simeq ln2 \times \frac{N.t}{S}$) where N is the number of 2β emmiter nuclei and S the number of recorded counts during time t (or the upper limit of double beta counts consistent with the observed background). In the case of taking for S the background fluctuation one has the so-called detector factor-of-merit or neutrinoless sensitivity which for source=detector devices reads $F_D = 4.17 \times 10^{26}(f/A)(Mt/B\Gamma)^{1/2}\varepsilon_\Gamma$ years where B is the background rate (c/keV kg y), M the mass of 2β emitter (kg), ε_Γ the detector efficiency in the energy bin Γ around $Q_{2\beta}$ (Γ = FWHM) and t the running time measurement in years (f is the isotopic abundance and A the mass number). The other guideline of the experimental strategy is to choose a 2β emitter of large nuclear factor

of merit $F_N = G_{0\nu} \mid M^{0\nu} \mid^2$, where the kinematical factor qualifies the goodness of the $Q_{2\beta}$ value and $M^{0\nu}$ the likeliness of the transition. Notice that the upper limit on $\langle m_\nu \rangle$ is given by $\langle m_\nu \rangle \leq \langle m_e \rangle / (F_D F_N)^{1/2}$, or in terms of its experimental and theoretical components
$\langle m_\nu \rangle \leq 2.5 \times 10^{-8} \times (A/f)^{1/2} \times (B\Gamma/Mt)^{1/4} \times \epsilon_\Gamma^{-1/2} \times G_{0\nu}^{-1/2} \times \mid M^{0\nu} \mid^{-1} eV$

4. Experimental Searches: Overview of Recent Results. The Germanium Case

The current status of the double beta decay searches is sketched in Table 9 where the main features, parameters and results of the experiments are summarized. From the list of emmiters and experiments quoted in Table 9 the germanium case has been chosen to illustrate in some detail a typical strategy in double beta searches.

There exist two experiments in operation looking for the double beta decay of ^{76}Ge. They both employ several kilograms of enriched ^{76}Ge (86%) in sets of detectors: the IGEX Collaboration experiment [16] (a set of three detectors of total mass 6.3 kg) in the Canfranc Underground Laboratory (Spain) and the Heidelberg/Moscow Collaboration experiment [17] (a set of five detectors amounting to 10.2 kg) running in Gran Sasso. Both experiments where designed to get the highest possible sensitivity to look for the neutrinoless double beta decay of the ^{76}Ge: a large amount of the Ge-76 isotope, in detectors of good energy resolution and very low radioactive background.

In the case of IGEX, the quest for an ultralow background started with a thorough radiopurity screening of the materials to be used in the detectors and in the inner components of the shielding. A thick passive shield (of about roughly 50 cm of lead) was employed. A continuous flux of clean nitrogen gas was injected into the shield to evacuate the radon. On the other hand an active veto shield rejected muon induced events and a neutron shield completed the barrier against external sources of background. This shielding will be described later on. A final step in the reduction was obtained through the event selection via Pulse Shape Discrimination (PSD) explained later on.

The FWHM energy resolutions of the three 2 kg IGEX detectors at 1333-keV are 2.16, 2.37, and 2.13 keV, and the energy resolution of the summed data integrated over the time of the experiment was $\sim$ 4keV at Q=2039 keV. The detectors cryostats were made in electroformed copper. The cooper part of the cryostat were produced by special techniques to eliminate Th and Ra impurities. All other components were made from radiopure materials. The first stage FET (mounted on a Teflon block a few centimeters apart from the inner contact of the crystal) was shielded by 2.6 cm of 500 y old lead to reduce the background. Also the protective cover of the FET and the glass shell of the feedback resistor were removed for such purpose. Further stages of amplification were located 70 cm away from the crystal. All the detectors have preamplifiers modified for pulse shape analysis (PSD) for background identification. Finally, special care was put in maintain a long-term stability in gain, resolution, noise, count rate, PSD signal, etc.

The data acquisition system had an independent spectroscopy chain for each Ge detector. The threshold was set to 1.5 MeV in plastic scintillators to register low energy deposits of muons and to 100 keV in Ge detectors to avoid unnecessary high count rates. For each Ge event, the time elapsed since run started ($100\mu s$ ticks), the time elapsed since last veto signal ($20\mu s$ ticks), the ADC channel numbers (range 0-8191, $\sim$ 1 keV/ch) and the scope trace with pulse shape (500 points, 2ns/point) were recorded. As far as stability on gain and resolution the energy shifts at $\sim$ 1.3 MeV are smaller than 0.5 keV (typically 0.3 keV) over 2 months and the energy resolution at $\sim$ 1.3 MeV was 2.2 - 2.5 keV over 2 months. The integrated resolution over $\sim$ 900 days of data spread to $\sim$ 3.5 keV.

The IGEX setup has been running in the Canfranc Underground Laboratory (Spain) at 2450 m.w.e. Special attention deserves the heavy shielding which was developed for this experiment. It consist of a large shielding enclosing tightly the set of detectors. First there is an innermost shield of 2.5 tons ($\sim$ 60 cm cube) of archaeological lead (2000 yr old) –having a ^{210}Pb(^{210}Bi) content of $<$ 0.01 Bq/kg–, where the 3 large detectors are fitted into precision-

Table 2
Theoretical half-lives $T^{2\nu}_{1/2}$ in some representative nuclear models.

	Theory							
	SM			QRPA		1^+D	OEM	MCM
	[8]	[18]	[14]	[7]	[5]	[19]	[15]	[20]
^{48}Ca(10^{19}y)	2.9	7.2	3.7					
^{76}Ge(10^{21}y)	0.42	1.16	2.2	1.3	3.0		0.28	1.9
^{82}Se(10^{20}y)	0.26	0.84	0.5	1.2	1.1	2.0	0.88	1.1
^{96}Zr(10^{19}y)				0.85	1.1			.14-.96
^{100}Mo(10^{19}y)				0.6	0.11	1.05	3.4	0.72
^{116}Cd(10^{19}y)					6.3	0.52		0.76
^{128}Te(10^{24}y)	0.09	0.25		55	2.6	1.4		
^{130}Te(10^{21}y)	0.017	0.051	2.0	0.22	1.8	2.4	0.1	
^{136}Xe(10^{21}y)			2.0	0.85	4.6			
^{150}Nd(10^{19}y)					0.74			

machined holes to minimize the empty space around the detectors available to radon. Nitrogen gas evaporated from liquid nitrogen, is forced into the remaining free space to minimize radon intrusion. Surrounding the archaeological lead block there is a 20-cm thick layer of low activity lead ($\sim$ 10 tons), sealed with plastic and cadmium sheets. A cosmic muon veto and a neutron shield (20 cm thick made from polyethylene bricks enlarged later on up to 40 cm plus 20 cm of borated water, placed externally) close the assembly.

The energy spectrum of one IGEX detector is shown in the Figure 1. Most of the background in the relevant $Q_{2\beta}$ region of 2039 keV is accounted for by cosmogenic activated nuclei (^{68}Ge and ^{60}Co). The background recorded in the energy region between 2.0 and 2.5 MeV is about 0.2 c/keV kg y prior to PSD. Background reduction through Pulse Shape Discrimination successfully eliminate multisite events, characteristic of non-2β events.

The rationale for PSD is quite simple: in large intrinsic Ge detectors, the electric field increases by a factor or more than 10 from the inner conductor to the outer conductor, which are almost 4 cm apart. Electrons and holes take 300 - 500 ns to reach their respective conductors. The current pulse contributions from electron and holes are displacement currents, and therefore dependent on their velocities and radial positions. Accordingly, events occurring at a single site ($\beta\beta$-decay events for example) have associated current pulse characteristics that reflect the position in the crystal where the event occurred. More importantly, these single-site event frequently have pulse shapes that differ significantly from those due to the most dominant background events that produce electron-hole pairs at several sites by multi-Compton-scattering process, for example. Consequently, pulse-shape analysis can be used to distinguish between these two types of energy depositions.

To develop PSD techniques it is helpful to work with a signal as close as possible to the displacement current of the detector. This allows the development of algorithms that do not depend strongly on the preamplifier electronics in use. To this end, the transfer function of the preamplifier and associated front-end stage has been measured for each detector. This allows the reconstruction of the displacement current and easy comparison to computed pulse shapes.

Double-beta decay events will deposit energy at a single site in a detector. Most background events will deposit energy at several sites. Our models of the structure of the current pulse reveal that single-site events will exhibit only one or two features, or "lobes", in more than 97% of the cases. Multiple site events will most often exhibit more than two lobes.

One PSD technique is to reject pulses having more than two significant lobes or peaks. To detect lobes, a "Mexican-hat" filter of the proper width is applied to the pulse. This robust method

is nearly model-independent. Some multiple-site events may show only one or two lobes and will not be rejected by this technique. Use of this PSD method results in the rejection of 60%–80% of the IGEX background in the energy interval 2.0–2.5 MeV, down to less than $\sim$ 0.07c/keV.kg.y.

The IGEX data histrograms for the $0\nu\beta\beta$ region are shown in Fig. 2. The combined energy resolution is 4 keV. PSD has only been applied to a fraction of data and so two analysis were made, with and without inclusion of PSD. In the Fig. 2, the light-gray area represents the complete data set corresponding to 116.75 fiducial mole-years (8.87 kg.y) and the dark-grey area represents the complete data set after the application of PSD (only 4.64 kg.y of data out of the total 8.87 kg.y have been Pulse Shape analyzed –2.74 kg.y of detector RG2 data, with rejection factor of 60.44% and 1.90 kg.y of detector RG3 data with a rejection factor of 76.54%–).

Table 3
IGEX Data bins for 8.87 kg.y in ^{76}Ge

E(low) keV	SSE data set	Complete data set
2020	2.9	2.9
2022	9.1	11.1
2024	3.4	4.4
2026	2.0	5.0
2028	4.6	7.6
2030	6.5	8.5
2032	2.3	5.3
2034	0.6	1.6
2036	0.0	3.0
2038	2.0	4.0
2040	1.5	2.5
2042	5.5	5.5
2044	6.0	7.0
2046	1.7	3.7
2048	5.3	6.3
2050	3.4	4.4
2052	4.6	6.6
2054	5.0	8.0
2056	0.6	1.6
2058	0.1	0.1
2060	4.3	6.3
Expected counts	13.6	20.08
Observed counts	4.1	11.1
Upper limit A (90%CL)	3.1	4.3
ln2.Nt/A	1.57×10^{25}y	1.13×10^{25}y

Table 3 shows the IGEX data for the mentioned exposure of 8.87 kg.y in ^{76}Ge (expressed as number of counts per 2 keV bin) in the region between 2020 and 2060 keV, for the two sets of 8.87 kg.y of data with (first column) and without (second column) application of PSD. Using the statistical estimator recommended by the Particle Data Group, 90% C.L. half-life lower bounds of $T^{0\nu}_{1/2} \geq 1.13 \times 10^{25} y$ for the complete data set (dashed line) and of $T^{0\nu}_{1/2} \geq 1.57 \times 10^{25} y$ for the complete data set with PSD (solid line) are obtained (see Table 3) [16]. Accordingly, the limit on the neutrino mass parameter is 0.38–1.55 eV for one data set and 0.33–1.31 eV for the other data set as shown in Table 4. The uncertainties originate from the spread in the calculated nuclear structure parameters.

Table 4
$\langle m_\nu \rangle$ bounds resulting from IGEX ($T^{0\nu}_{1/2} \geq 1.57 \times 10^{25} y$) according to various representative nuclear models.

		$\langle m_\nu \rangle$(eV)	
		Complete	SSE
$F_N(y^{-1})$	Model	Data set	Data set
1.56×10^{-13}	WCSM[8]	0.38	0.33
9.67×10^{-15}	QRPA[7]	1.55	1.31
1.21×10^{-13}	QRPA[10]	0.44	0.37
1.12×10^{-13}	QRPA[5]	0.45	0.39
1.41×10^{-14}	SM[14]	1.28	1.09

Data from one of the IGEX detectors, RG–3 –which went underground in Canfranc several years ago– corresponding to 291 days, were used to set a value for the 2ν-decay mode half-life by simply subtracting the MC-simulated background. Figure 3-a shows the best fit to the stripped data corresponding to a half-life $T^{2\nu}_{1/2} = (1.45 \pm 0.20) \times 10^{21}$ y, whereas Figure 3-b shows how the experimental points fit the double beta Kurie plot (see Ref. [21]).

The Heidelberg/Moscow experiment operates five p-type HPGe detector of enriched ^{76}Ge (86%) with a total active mass 0f 10.96 kg, corresponding to 125.5 mol of ^{76}Ge. A detailed description

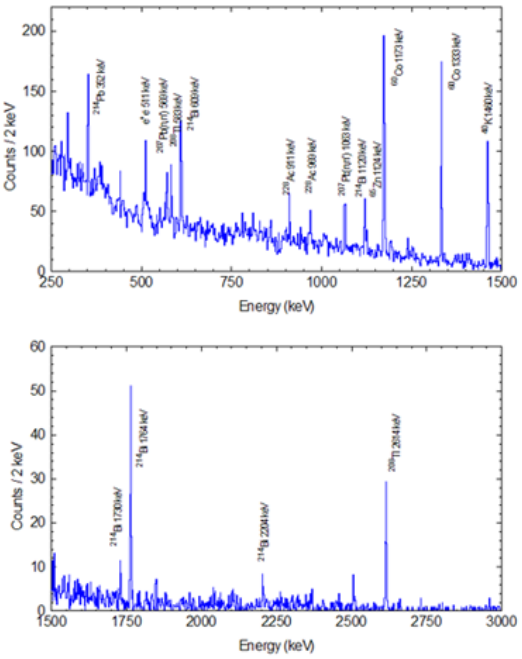

Figure 1. Energy spectrum of one IGEX detector (RG-II) for exposure of 2.75 kg y.

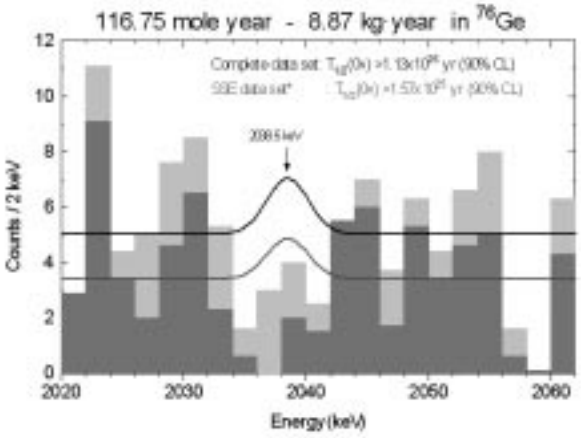

Figure 2. Two-electron summed energy spectrum of the IGEX experiment around $Q_{2\beta} = 2039$ keV region

of the experiment is given in Ref. [17] and references therein.

Figure 4 shows the recorded background spectrum of the detectors of the H/M experiment corresponding to an exposure of 47.4 kg.y compared with the MonteCarlo simulation of the background. After substraction, the resulting half-life for the $2\nu\beta\beta$-decay at 68% C.L. is

$$T^{2\nu}_{1/2} = \{1.55 \pm 0.01(stat)^{+0.19}_{-0.15}(syst)\} \times 10^{21}\text{y}$$

in agreement with the 1998 IGEX result [21].

To derive the neutrinoless decay half-life limit from the H/M experiment, the raw data of all five detectors as well as data with pulse shape analysis are considered (see Fig 5). No indication for a peak at the Q-value $0\nu\beta\beta$-decay is seen in none of the two data sets (the first 200 d of measurement of each detector were suppressed, because of possible interference with the cosmogenic ^{56}Co). Data prior to PSD show a background around the Q-value of (0.19 ± 0.1)c/keV.kg.y similar to that of IGEX (0.2c/keV.kg.y).

The average energy resolution at the $Q_{2\beta}$ value is (4.23 ± 0.14)keV. The set of data analyzed with PSD correspond to 35.5 kg.y of exposure and its background in the energy region between 2000.2080 keV is (0.06 ± 0.01)counts/(keV.kg.y). Following the method proposed of PDG, the limit on the half-life is [17]

$$T^{0\nu}_{1/2} \geq 1.9 \times 10^{25} \text{ y} \qquad 90\% \text{ C.L.}$$

After a new statistical analysis of the same set of data, some of the authors of the H/M collaboration conclude [22] that there exists evidence of a neutrinoless double beta peak. That result, of scarcely 2σ statistical significance, has been very widely contested [23,24].

In the case of other emitters, from the neutrinoless half-live limits given in Table 5 one can derive Majorana neutrino mass bound according to the nuclear model of his choice. Table 7 shows the range of bounds derived from the most sensitive experiment. Table 6 shows the neutrinoless half-lives theoretical predictions, in terms of $\langle m_\nu \rangle$.

Table 6
Neutrinoless half-lives in various Theoretical Models (for the $\langle m_\nu \rangle$ term) $T^{0\nu}_{1/2}\langle m_\nu \rangle^2$ values are given in 10^{24} (eV)^2 y.

	^{76}Ge	^{82}Se	^{100}Mo	^{128}Te	^{130}Te	^{136}Xe	^{150}Nd	^{116}Cd	^{48}Ca
Weak Coupl. SM [8]	1.67	0.58		4.01	0.16				
$g_A = 1.25 (g_A = 1)$	(3.3)	(1.2)		(7.8)	(0.31)				
Large Space SM [14]	17.5	2.39				12.1			6.25
QRPA [7]	14	5.6	1.9	15	0.66	3.3			
QRPA [6]	2.3	0.6	1.3	7.8	0.49	2.2	0.034	0.49	
QRPA [10]	2.15	0.6	0.255	12.7	0.52	1.51	0.045		
OEM [15]	2.75	0.704		12.6	0.723	4.29	0.056	0.583	
QRPA with [12]	18.4	2.8	350	150	2.1	2.8		4.8	28
(without) np pair. [11]	(3.6)	(1.5)	(3.9)	(19.2)	(0.86)		(4.7)	(2.4)	

Table 5
Limits on Neutrinoless Decay Modes

Emitter	*Experiment*	$T^{0\nu}_{1/2} >$	*C.L.%*
^{48}Ca	HEP Beijing	1.1×10^{22} y	68
^{76}Ge	MPIH/KIAE	1.9×10^{25} y	90
	IGEX	1.6×10^{25} y	90
^{82}Se	UCI	2.7×10^{22} y	68
	NEMO 2	9.5×10^{21} y	90
^{96}Zr	NEMO 2	1.3×10^{21} y	90
^{100}Mo	LBL/MHC/UNM	2.2×10^{22} y	68
	UCI	2.6×10^{21} y	90
	Osaka	6.5×10^{22} y	90
	NEMO 2	6.4×10^{21} y	90
^{116}Cd	Kiev	7×10^{22} y	90
	Osaka	2.9×10^{21} y	90
	NEMO 2	5×10^{21} y	90
^{130}Te	Milano	2.1×10^{23} y	90
^{136}Xe	Caltech/UN/PSI	4.4×10^{23} y	90
^{136}Xe	Rome	7×10^{23} y	90
^{150}Nd	UCI	1.2×10^{21} y	90

Table 7
Current best constraints on $|\langle m \rangle|$. Results

Experiment	$\lvert\langle m\rangle\rvert <$ (eV)
IGEX enrich. ^{76}Ge	$(0.33 \sim 1.35)$ (6.0kg)
H/M enrich. ^{76}Ge	$(0.35 \sim 1.05)$ (10.9kg)
MIBETA nat. ^{130}Te	$(0.85 \sim 2.1)$ (6.8kg)

Table 8
Expected best constraints on $|\langle m \rangle|$.

Experiment	$\lvert\langle m\rangle\rvert <$ (eV)
NEMO3 enrich. ^{100}Mo	0.1 (10kg)
CUORE nat. ^{130}Te	0.05 (1Ton)
EXO enrich. ^{136}Xe	0.02 (2Ton)
GEDEON-1 enrich. ^{76}Ge	0.04-0.10 (70kg)
GENIUS enrich. ^{76}Ge	0.01 (1Ton)
	0.001eV (10Ton)
MAJORANA enrich. ^{76}Ge	0.01 (500kg)
MOON enrich. ^{100}Mo	0.03 (2Ton)

5. Future Prospects: The Germanium Option

It has been made clear that the neutrinoless double beta decays are very rare phenomena which, if detected, will provide important evidences of a New Physics beyond the Standard Model of Particle Physics, and would have far-reaching consequences in Cosmology. The experimental achievements accomplished during the last decade in the field of ultra-low background detectors have lead to sensitivities capable to search for such rare events. To increase the chances of observing such rare events, however, large amounts of detector mass are mandatory, but keeping the other experimental parameters optimized.

The best Majorana neutrino effective mass bound obtained so far have been obtained with Ge diodes: $\langle m_\nu \rangle \leq$(0.3–1.3)eV (IGEX and H/M experiments). Extension of these experiments are being considered with the purpose of reaching the frontier of the 10 meV for the Majorana neutrino mass bound.

The achievement of 0.2 c/(keV.kg.y) (at 2MeV), in the raw background data of IGEX and H/M has been considered as a stationary limit whose reduction requires further and deeper in-

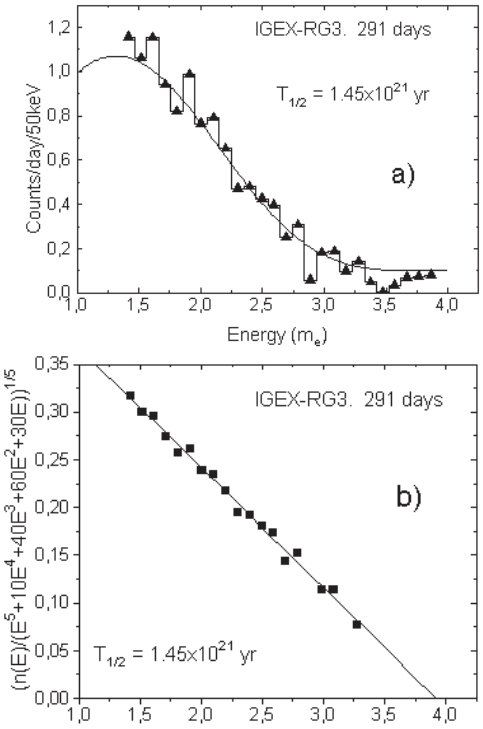

Figure 3. a) Best fit to the stripped data corresponding to a half-life $T^{2\nu}_{1/2} = (1.45\pm0.20)\times10^{21}$ y. b) Experimental points fit the double beta Kurie plot

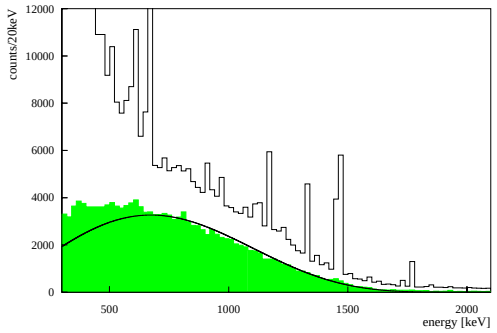

Figure 4. Energy spectrum of the five H/M detectors for 47.7 kg y of exposure.

vestigation. Starting from the IGEX background achievements, the main challenge of the future extended Ge experiments (besides using large quantities of the emitter nucleus) is to substantially improve the radiopurity of the detectors and components (both intrinsic and induced) and to suppress, as best as possible, the background originated from external sources. A final step in the reduction could then be obtained through pulse shape analysis (PSD) (a factor one third–one fourth) or by some new techniques.

The energy resolution, another important parameter in the search for a neutrinoless signal – which should appear as a peak at the two-electron summed energy at Q=2039 keV- is rather sharp in the case of Ge-diodes ($3 \sim 4$ keV integrated along long period of time), and so not too much progress can be expected. Needless to say that special care must be put in maintain a long-term stability in gain, resolution, noise, count rate, PSD signal, etc.

The success of the Germanium option in obtaining the most stringent bound to the Majorana neutrino effective mass, the mastering of the techniques in making Ge detectors, the ultra-low background achievements (in their raw data spectrum), their long-term stability, good energy resolution and reasonable nuclear factor of merit, make the Germanium option –with conventional Ge diodes- worth to be explored further, with improved experimental parameters, in new generation experiments, with the objective of reaching the 10-20 meV level for the Majorana neutrino effective mass bound, where recent data from solar and atmospheric neutrino experiments place the discovery potential of the neutrinoless double beta decay.

Extensions of the respective IGEX and Heidelberg/Moscow Ge-experiments to larger masses and hopefully lower backgrounds are the Majorana project [25] (500 kg of enriched ^{76}Ge) and the GEDEON proposal [26] (70 kg of ^{76}Ge in a first step, followed by larger masses in subsequent steps). Both proposals plan to use conven-

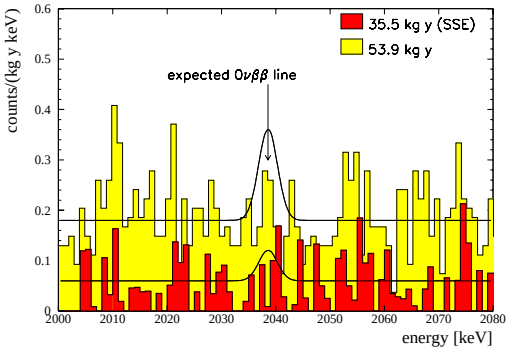

Figure 5. Two-electron summed energy spectrum of the H/M experiment around $Q_{2\beta}$=2039 keV region.

tional Ge-diodes although with modifications to improve substantially the background.

On the other hand, an extension of the H/M experiment is the GENIUS project [27], which plan to use 1 ton of naked Ge crystals embedded directly in liquid nitrogen in a cylinder container. There exists also a proposal called GEM which would locate 1 ton of naked HPGe diodes inside an spherical vessel containing ultrapure liquid nitrogen in a water shield (BOREXINO-CTF-like). Both experiments plan to reach a half-life limit of $T^{0\nu}_{1/2} \geq 10^{28}$ y, which would lead to a mass bound of 15 meV (in the case of using, for instance, one of the QRPA nuclear matrix element, i.e., $F^{0\nu}_N = 1.12 \times 10^{-13}$ y^{-1} for the Ge nuclear factor of merit [5].

The Majorana project [25] will extend significantly the IGEX mass (from 6.3 kg up to 500 kg of ^{76}Ge), and starts from the technical achievements of the IGEX detectors. It will use however new, commercially developed segmented Ge detectors and new Pulse Shape Discrimination (PSD) techniques developed after the completion of IGEX. It will use isotopically enriched germanium (86% in ^{76}Ge) as in IGEX, in an ensemble of 200 detectors of about 2.5 kg each. Each detector is segmented into 12 electrically-independent volumes, each of which will be read-out with the new designed PSD system. The two new ingredients (besides the larger mass of germanium), i.e., the segmentation and the new PSD, are supposed to reduce substantially the intrinsic background (mainly cosmogenic) of the IGEX detectors, down to a 3.7% only (respectively 0.265 through PSD and 0.138 due to segmentation) of the raw IGEX background in the $Q_{2\beta}$=2039 keV energy region (B=0.2 c/(keV.kg.y)), down to 7.5×10^{-3} c/(keV.kg.y). Capitalizing the fact that the IGEX background in this region was accounted for as the decay of cosmogenic induced isotopes in the Germanium (^{68}Ge, half-life of 271 days and ^{60}Co, half-life 5.7 years), the proponents of the Majorana experiment anticipate that taking special care in the fabrication and transport of the detectors and accounting for the decay of the cosmogenic induced activities along the ten years of running time of the experiment, a further suppression factor of about 20 could be, presumably, obtained, and so the background expected would be about B=5×10^{-4} c/(keV.kg.y) (corrected by the efficiency of the PSD and segmentation cuts).

With the inputs Mt=5000 kg y, B=5×10^{-4} c/(keV.kg.y), Γ=3.5 keV Majorana would obtain a half-life limit of $T^{0\nu}_{1/2} \geq 4.2 \times 10^{28}$ y which provide bounds for the Majorana neutrino mass ranging from $\langle m_\nu \rangle \sim (20 - 70)$ meV according to the nuclear matrix elements employed.

The GEDEON (GErmaniun DEtector in ONe cryostat) proposal [26] is also an extension of the IGEX experiment, in various steps including, in a first step, the use of natural abundance germanium in a search for WIMPs. It also relies in the IGEX technology, putting the emphasis mainly in the elimination of the cosmogenic induced activity of the detectors, instead of in the read-out. It will consist in sets of germanium crystals of 2.5 kg each arranged in cells containing 28 Ge crystals (four planes of seven Ge diodes per plane, in only one cryostat (cell-unit), made in copper electroformed underground). A first cell, in natural isotopic abundance germanium will test the performances of the set-up and look for WIMPs. Then the inclusion of enriched ^{76}Ge detectors in cells of 70 kg would be implemented in successive steps. The shielding will be made from Roman lead (inner) and low activity lead (outer), in much

the same way as in IGEX. After that shield, neutron shieldings of polyethylene and borated water as well as muon vetos would complete the set-up. The experiment will be installed in the new Canfranc Underground Laboratory. A quantitative study by MC simulations of the GEDEON intrinsic background is now in progress; for instance, a background of 0.002 c/keV/kg/day is reasonably expected in the low energy region (Ref.[26]). Studies of the background in the 2 MeV region are in course.

GEDEON will use conventional (not-segmented) Ge detectors with improved PSD. However, the main emphasis of this proposal will be put in avoiding almost completely the activation of the crystals and components. A significant background reduction is expected to be obtained in GEDEON with respect to IGEX due to the growing of the detector's crystals in the underground site itself. Also the electroformed copper cryostats will be made underground, whereas the multiple melting of archaeological lead and the machining of bricks for shielding will be performed, in much the same way as in IGEX, but underground. Clean rooms will be used for assembling and mounting the detectors. The almost suppression of the cosmogenic activation could lower the levels of raw background by a conservative factor of 50, down to B=4×10^{-3} c/(keV.kg.y) from the starting "plateau" value of 0.2 c/(keV.kg.y) of IGEX, that will be further reduced by PSD analysis by a factor of 4, down to B$\sim 1\times10^{-3}$ c/(keV.kg.y). With this value, and using the neutrinoless sensitivity expression for germanium,

$$S^{0\nu}_{1/2} \sim 4.94\times10^{24}(\mathrm{Mt/B\Gamma})^{1/2} \text{ years}$$

one would obtain in the case of M=70 kg, Γ=3 keV, t=5 years a half-life sensitivity bound of $S^{0\nu}_{1/2} \sim 1.7\times10^{27}$ y from where a bound of $\langle m_\nu\rangle < 40$ meV could be obtained by using the nuclear matrix element calculation of [5]. Somehow higher values would be obtained with other nuclear matrix elements (or nuclear-factor-of-merit) from Table 1.

The Phase I of GEDEON could be considered as an intermediate step ($\langle m_\nu\rangle \geq (0.04 \sim 0.1)$ eV) conventional-Ge experiment. The addition of more mass of emitters will provide improved bounds, which could reach a sensitivity of $S^{0\nu}_{1/2} \sim 10^{28}$ y, with a set of five cells in 5 years. GEDEON offers as a bonus that the absence of cosmogenic activation will permit to start the experiment with a very low background without need to wait for the cooling of activations.

In conclusion, the Germanium detectors/emitters, which have provided the best neutrino mass bounds, are a most valid option for future, next generation double beta decay experiments.

6. Conclusions and Outlook

The standard two-neutrino decay mode has been directly observed in several nuclei: ^{48}Ca, ^{76}Ge, ^{82}Se, ^{96}Zr, ^{100}Mo, ^{116}Cd and ^{150}Nd and others are under investigation (^{130}Te, ^{136}Xe) as summarized in Table 9. Limits on neutrinoless half-lives have been derived from that experiments (see the recent Reviews in Ref. [28]). Nuclear model calculations give still a large spread of prediction, and that translates into a broad uncertainty in the Majorana effective neutrino mass bound derived from the results.

Data from the most sensitive experiments on neutrinoless double beta decay lead to the limit $\langle m_\nu\rangle < 0.3 - 1.3$ eV for the effective neutrino mass, according to the nuclear model. The Ge experiments provide the stringest bound to the neutrino mass parameter and they seem to offer, for the next future, the best prospectives to reach the lowest values of $\langle m_\nu\rangle$. There exist obviously other emitters and techniques for large next generation double beta decay experiments.

Currently running or nextcomming experiments (say, respectively, NEMO 3 and CUORICINO) will explore effective neutrino masses down to about 0.1—0.3 eV. To increase the sensitivity it is necessary to go to larger source masses and reduce proportionally the background, like the projects mentioned in Section 5. That would bring the sensitivity to neutrino mass bounds down to a few 10^{-2}eV. Table 8 give a simple look to the expectations of some of these experiments, schematically described in Table 9.

7. ACKNOWLEDGEMENTS

We thak Susana Cebrián for her collaboration in the GEDEON proposal and, in particular, for the MC estimation of the background, and Frank Avignone for information and discussion on the Majorana project. The financial support of CICYT (Spain) under contract AEN99-1033 is acknowledged.

Table 9: Synopsis of Double Beta Decay Searches

	Method	**Results**
	^{48}Ca→^{48}Ti Q=4276keV	
HEP Inst. Beijing	Large scint. crystals of natural CaF_2(43 gr of Ca^{48})	$T^{0\nu}_{1/2} \geq 1.14 \times 10^{22}$y (68%) $T^{0\nu\chi}_{1/2} > 7.2 \times 10^{20}$y (90%)
UCI Hoover Damm 260 mwe	Helium TPC (atm. press.). Central powder source $CaCO_3$ m=42.2 gr and m=10.3 g (73% enriched) efficiency $\sim 10\%$	$T^{2\nu}_{1/2} = (4.3^{+2.4}_{-1.1} \pm 1.4) \times 10^{19}$y
	^{76}Ge→^{76}Se Q=2039keV	
Heidelberg/Moscow Gran Sasso 3330 mwe	Set of large (enriched) Ge detectors 11.5 kg (10.9 kg fiducial) (2001)	$T^{2\nu}_{1/2} = (1.55 + 0.01^{+0.19}_{-0.15}) \times 10^{21}$y $T^{0\nu}_{1/2} \geq 1.9 \times 10^{25}$y (90%) $T^{0\nu\chi}_{1/2} \geq 6.4 \times 10^{22}$y (90%)
IGEX Canfranc 2450 mwe	Set of large (enriched) Ge detectors 6.3 kg (6.0 kg fiducial)(1998)	$T^{2\nu}_{1/2} = (1.45 \pm 0.15) \times 10^{21}$y $T^{0\nu}_{1/2} \geq 1.6 \times 10^{25}$y (90%)
	^{82}Se→^{82}Kr Q=2992keV	
UCI Hoover Damm 260 mwe	Helium TPC (atm. press.). Central powder source (few grams) Efficiency $\sim 10\%$)	$T^{2\nu}_{1/2} = (1.08^{+0.26}_{-0.06}) \times 10^{20}$y $T^{0\nu}_{1/2} \geq 2.7 \times 10^{22}$y (68%) $T^{0\nu\chi}_{1/2} \geq 1.6 \times 10^{21}$y (68%)
NEMO 2 Frejus 4800 mwe (1998)	Electron tracking device, Geiger cells. V=1 m^3, Eff 2% External plastic calorim. Vertical central source enr. 97% (156 g) and nat. (134 g)	$T^{2\nu}_{1/2} = (0.83 \pm 0.09 \pm 0.06) \times 10^{20}$y $T^{0\nu}_{1/2} \geq 9.5 \times 10^{21}$y (90%) $T^{0\nu\chi}_{1/2} \geq 2.4 \times 10^{21}$y (90%)
Heidelberg	Geochemical	$T_{1/2} = (1.30 \pm 0.05 \times 10^{20}$y
Missouri	Geochemical	$T_{1/2} = (1.0 \pm 0.4 \times 10^{20}$y
	^{100}Mo→^{100}Ru Q=3351keV	
INR Baksan 660 mwe	Porportional chamber plus plasic scint. Powdre/source interleaved. 46g (90% enriched)	$T^{2\nu}_{1/2} = (3.3^{+0.2}_{-0.1}) \times 10^{18}$y
LBL Mt. Hol. UNM (Consil) 3300 mwe	Stack of semiconductors. 60g g(97% enriched)	$T^{2\nu}_{1/2} = (7.6^{+2.2}_{-1.4}) \times 10^{18}$y $T^{0\nu}_{1/2} \geq 2.2 \times 10^{22}$y (68%)
ELEGANTS V Osaka (Kamioka) 2700 mwe	Electron tracking det. Drift chambers, plastic scint. NaI modules. Eff$\sim 11\%(2\nu), 19\%(0\nu)$ Enriched 104g (94.5%) and nat. 171g	$T^{2\nu}_{1/2} = (1.15^{+0.30}_{-0.28}) \times 10^{19}$y $T^{0\nu}_{1/2} \geq 6.5 \times 10^{22}$y (90%) $T^{0\nu\chi}_{1/2} \geq 5.4 \times 10^{21}$y (68%)
UCI. Hoover Damm 260 mwe	Helium TPC (atm. press.) Central powdre source Enriched 8g (97.4%)	$T^{2\nu}_{1/2} = (1.16^{+0.34}_{-0.08}) \times 10^{19}$y $T^{0\nu}_{1/2} \geq 2.6 \times 10^{21}$y (90%)
	Enriched 16.7g (97.4%) Eff$\sim 10\%(2\nu), 11\%(0\nu)$	$T^{2\nu}_{1/2} = (6.82^{+0.38}_{-0.53} \pm 0.68) \times 10^{18}$y $T^{0\nu}_{1/2} \geq 1.23 \times 10^{21}$y (90%) $T^{0\nu\chi}_{1/2} \geq 3.31 \times 10^{20}$y
NEMO 2 Frejus 4800 mwe	Electron tracking detector Enriched 172g (98.4%). Nat. 163g Eff. $\sim$ few percent	$T^{2\nu}_{1/2} = (0.95 \pm 0.04 \pm 0.09) \times 10^{19}$y $T^{0\nu}_{1/2} \geq 6.4 \times 10^{21}$y (90%) $T^{0\nu\chi}_{1/2} \geq 5.0 \times 10^{20}$y (90%)

Table 9: (Continued)

	Method	**Results**
	^{96}Zr→^{96}Mo Q=3351keV	
Kawashima et al.	Geochemical. $1,7 \times 10^9$y old Zircon	$T_{1/2} = (3.9 \pm 0.9) \times 10^{19}$y
NEMO 2 Frejus	Electron tracking detector. Central vertical source	$T^{2\nu}_{1/2} = (2.1^{+0.8}_{-0.4} \pm 0.2(syst)) \times 10^{19}$y
4800 mwe	Enriched 20.5g (57.3%) ZrO_2. Nat 18.3g	$T^{0\nu}_{1/2} \geq 1.3 \times 10^{21}$y (90%)
	t=10357 h	$T^{0\nu\chi}_{1/2} \geq 3.5 \times 10^{20}$y (90%)
	^{116}Cd→^{116}Sn Q=2804keV	
ELEGANTS V	Electron tracking det. Drift chambers, plastic scint.	$T^{2\nu}_{1/2} = (2.6^{+0.9}_{-0.5} \pm 0.35) \times 10^{19}$y
Osaka (Kamioka)	Enriched 91.1g (90.7%). Nat 88.5g, Eff. 8%	$T^{0\nu}_{1/2} \geq 5.44 \times 10^{21}$y (90%)
NEMO 2 Frejus	Electron tracking detector. Central vertical source	$T^{2\nu}_{1/2} = (3.75 \pm 0.35 \pm 0.21) \times 10^{19}$y
4800 mwe	Enriched 152g (93.2%). Nat 143g	$T^{0\nu}_{1/2} \geq 5.0 \times 10^{21}$y (90%)
	Efficiency $\sim 1.7\%$	$T^{0\nu\chi}_{1/2} \geq 1.2 \times 10^{21}$y (90%)
INR Kiev	Cadmium Tungstate scint. crystal	$T^{2\nu}_{1/2} = (2.7^{+0.5+0.9}_{-0.5-0.6}) \times 10^{19}$y
(Solotvina) 1000 mwe	$CdWO_4$ enriched 83% and natural	$T^{0\nu}_{1/2} \geq 7 \times 10^{22}$y (90%)
	Efficiency 83.5% (0ν)	$T^{0\nu\chi}_{1/2} \geq 1.2 \times 10^{21}$y (90%)
	^{128,130}Te→^{128,130}Xe Q=867/2529keV	
Washington. St Louis	Geochemical. 4g. 2×10^9y old Tellurium ore	$T^{130}_{1/2}/T^{128}_{1/2} = (3.52 \pm 0.11) \times 10^{-4}$ $T^{130}_{1/2} = (2.7 \pm 0.1) \times 10^{21}$y $T^{128}_{1/2} = (7.7 \pm 0.4) \times 10^{24}$y $T^{130}_{1/2}$ controversial. Instead $(7 - 27) \times 10^{20}$y $T^{0\nu}_{1/2}(128) > 6.9 \times 10^{24}$y $T^{0\nu}_{1/2}(130) > 2.54 \times 10^{21}$y
Missouri	Geochemical	$T^{130}_{1/2} = (0.75 \pm 0.3) \times 10^{21}$y $T^{128}_{1/2} = (1.4 \pm 0.4) \times 10^{24}$y
	1991. 5g 3×10^{19}y old Tellurium ore	$T^{130}_{1/2}/T^{128}_{1/2} = (4.2 \pm 0.8) \times 10^{-4}$
Heidelberg	Geochemical	$T^{130}_{1/2} = (1.5 - 2.8) \times 10^{21}$y $T^{128}_{1/2} > 5 \times 10^{24}$y
Takaoka et al.	Geochemical	$T^{130}_{1/2} = (7.9 \pm 1.0) \times 10^{20}$y $T^{128}_{1/2} = (2.2 \pm 0.3) \times 10^{24}$y from $T^{130}_{1/2}/T^{128}_{1/2} = (3.5 \pm 0.11) \times 10^{-4}$
recommended values:	$T^{130}_{1/2} = 8 \times 10^{20}$y ; $T^{128}_{1/2} = (2 \times 10^{24}$y	
	^{130}Te→^{130}Xe Q=2529keV	
Milan	Cryogenic exp. Bolometers of TeO_2	
MIBETA	Natural Te (34%). NTD sensors. Eff $\sim 100\%$	
(Gran Sasso)	73 g at 15 mK	$T^{0\nu}_{1/2} \geq 2.5 \times 10^{21}$y (90%)
	334 g at 10 mK	$T^{0\nu}_{1/2} \geq 2.8 \times 10^{22}$y (90%)
	4x330 g at 10 mK	$T^{0\nu}_{1/2} \geq 2.4 \times 10^{22}$y (90%)
	20x340 g	$T^{0\nu}_{1/2} \geq 2.1 \times 10^{23}$y (90%)
		$T^{0\nu}_{1/2}(^{128}Te \geq 1.7 \times 10^{22}$y (90%)

Table 9: (Continued)

	Method	**Results**
	^{136}Xe→^{136}Ba Q=2467keV	
Caltech/Neuchatel/PSI	Xe TPC (enr. 62.5%) at 5 bar. Fiducial 180 l. 24.4 mol	$T^{2\nu}_{1/2} \geq 5.5 \times 10^{20}$y (90%)
Gothard 3000mwe	(3.3 kg of ^{136}Xe) Global eff. 22%, Γ(2480 keV)∼ 6.6%	$T^{0\nu}_{1/2} \geq 4.4 \times 10^{23}$y (90%)
	Calorimeter and tracking detector at the same time	$T^{0\nu\chi}_{1/2} \geq 7.2 \times 10^{21}$y (90%)
Rome 2 (Gran Sasso)	Xenon chamber, Enriched source (2001)	$T^{0\nu\chi}_{1/2} \geq 7 \times 10^{23}$y
	^{150}Nd→^{150}Sm Q=3368keV	
UCI. Hoover Damm	Helium TPC (atm. press.) Central powder source	$T^{2\nu}_{1/2} = (6.75^{+0.37}_{-0.42} \pm 0.68) \times 10^{18}$y
260 mwe	Source 15.5 g of Nd_2O_3 enr.(91%). 1200 Gauss	$T^{0\nu}_{1/2} \geq 1.22 \times 10^{21}$y (90%)
	Efficiency ∼ 11%$(0\nu, 2\nu)$	$T^{0\nu\chi}_{1/2} \geq 2.82 \times 10^{20}$y (90%)
ITEP	CH_4 TPC (atm. press.). 800 Gauss. Prototype 0.3m^3	$T^{2\nu}_{1/2} = (1.88^{+0.69}_{-0.37} \pm 0.19) \times 10^{19}$y
at sea level	40 g of ^{150}Nd (92% enr.) and nat. 2.5 g of ^{150}Nd	$T^{0\nu}_{1/2} \geq 2.1 \times 10^{20}$y (90%)
and in Baksan	Efficiency ∼ 3%	$T^{0\nu\chi}_{1/2} \geq 1.7 \times 10^{20}$y (90%)
	^{238}U→^{238}Pu Q=1437keV	
Chicago/	Radiochemical experiment. Milking to get 5.5 MeV α's	$T_{1/2} = (2.0 \pm 0.6) \times 10^{21}$y
Santa Fe/	from ^{238}Pu (90y). Source 8.47g uranyl nitrate	$T^{0\nu}_{1/2} > 0.84 \times 10^{21}$y
Los Alamos	Ingrowth time: 33 y	$T^{0\nu\chi}_{1/2} > 0.8 \times 10^{21}$y
	^{244}Pu→^{244}Cm Q=1352keV	
Lawrence	Radiochemical experiment. Milking to get 5.8MeVα's	$T_{1/2} \geq 1.1 \times 10^{18}$y (95%)
Livermore	from ^{244}Cm (18y). Source 1.5g	$T^{0\nu}_{1/2} > 1.1 \times 10^{18}$y
National Lab.	Ingrowth time: 1.08 y	$T^{0\nu\chi}_{1/2} > 1.1 \times 10^{18}$y

REFERENCES

1. J. Schechter, J.W.F. Valle, Phys. Rev. D 25 (1982) 2951.
2. B. Kayser et al., "New and Exotic Phenomena", Ed. O. Facker, Editions Frontieres 1987, p. 349, W.C. Haxton, G.J. Stephenson Jr., Prog. Part. Nucl. Phys. 12 (1984) 409.
3. S. Pascoli, S. T. Petcov, [hep-ph/0205022].
4. M. Doi, T. Kotani, E. Takasugi, Progr. Theor. Phys. Suppl. 83 (1985) 1.
5. QRPA. A. Staudt et al, Europhys. Lett. 13 (1990) 31).
6. QRPA. T. Tomoda, Rep. Prog. Phys. 54 (1991) 53.
7. QRPA. P- Vogel et al., Phys. Rev: Lett. 57 (1986) 3148. Phys. Rev. C 37 (1988) 73. M. Moe and P. Vogel, Ann. Rev. Nucl. Part. Sci. 44 (1994) 247.
8. Weak Coupling SM. Haxton et al, Prog. Part. Nucl. Phys. 12 (1984) 409 and Nucl. Phys. B 31 (Proc. Suppl.) (1993) 82, Phys. Rev. D 26 (1982) 1085.
9. Generalized seniority. J. Engel and P. Vogel, Phys. Rev: Lett. B 225 (1989) 5.
10. QRPA. O. Civitarese, A. Faessler, T. Tomoda, Phys. Lett. B 194 (1987) 11. T. Tomoda, A. Faessler, Phys. Lett. B 199 (1987) 473. J. Suponen and O. Civitarese, Phys. Rev. C 37 (1994) 3055. See also T. Tomoda, Rep. Prog. Phys. 54 (1991) 53.
11. QRPA without pn pairing. Pantis et al, Phys. Rev. C 53 (1996) 695.
12. QRPA with pn pairing. Pantis et al, Phys. Rev. C 53 (1996) 695.
13. A. Staudt, Kuo and H. Klapdor, Phys. Rev. C 46 (1992) 871.
14. Large basis SM. E. Caurier et al., Phys. Let.. B 252 (1990) 13 and Erratum, Phys. Rev. C 50 (1994) 223. E. Caurier et al, Phys. Rev. Lett. 77 (1996) 54. Retamosa et al, Phys. Rev, 51 (1995) 371. A. Poves et al, Phys. Lett. B 361 (1995) 1.
15. Operador Expansion Model. J. G. Hirsh et al. Nucl. Phys. A 589 (1995) 445. C. R. Ching et al, Phys. Rev. C 40 (1984) 304. X. R. Wu et al, Phys. Lett. B 272 (1991) 169, Phys Lett. B 276 (1992) 274.
16. C. E. Aalseth et al, Phys. Rev. C 59 (1999) 2108. D. González et al, Nucl. Phys. B (Proc. Suppl.) 87 (2000) 278. C. E. Aalseth et al, Phys. Rev. D 65 (2002) 092007.
17. M. Gunther et al, Phys. Rev. D 55 (1997) 54. H. V. Klapdor-Kleingrothaus et al, Eur. Phys. J. A 12 (2001) 147.
18. W.C. Haxton, Nucl. Phys. B (Proc. Suppl.) 31 (1993) 82.
19. J. Abad, A. Morales, R. Núñez-Lagos, A.F. Pacheco, Ann. Fis. A 80 (1984) 9; J. Phys. C3 Suppl. 45 (1984) 147.
20. J. Suhonen and O. Civitarese, Phys. Rep. 300 (1998) 123.
21. A. Morales, Nucl. Phys. B (Proc. Suppl.) 77 (1999) 335.
22. H. V. Klapdor-Kleingrothaus et al, Mod. Phys. Lett. A 16 (2001) 2409.
23. F. Feruglio et al, [hep-ph/0201291].
24. C. Aalseth et al, Mod. Phys. Lett. A (2002), [hep-ex/0202018].
25. C. Aalseth et al, [hep-ex/0201021].
26. A. Morales et al., GEDEON: Set of Ge diodes in a single cryostat for 2β and WIMP searches, Preliminary Study for Submission to CICYT (Spain), January 1999. A. Morales, Proceedings of the 29^{th} International Meeting on Fundamental Physics, Sitges (Barcelona), Feb.2001.)
27. H. V. Klapdor-Kleingrothaus et al, J. Phys. G. Nucl. Part. Phys. 24 (1998) 483.
28. Recent Experimental Reviews are: A. Morales, Nucl. Phys. Proc. Suppl. **77** (1999) 335 [hep-ph/9809540]; H. Ejiri, Nucl. Phys. Proc. Suppl. **91** (2001) 255. E. Fiorini, Nucl. Phys. Proc. Suppl. **91** (2001) 262 and O. Cremonesi, Neutrino 2002, to be published in Nucl. Phys. (Proc. Suppl.) 2003.